

# NGC 5252 – a Liner undercover<sup>★</sup>

A.C. Gonçalves, P. Véron, and M.-P. Véron-Cetty

Observatoire de Haute-Provence (CNRS), F-04870 Saint Michel l'Observatoire, France

Received 8 December 1997 / Accepted 4 February 1998

**Abstract.** Ground based long slit spectroscopic observations of the nuclear region of NGC 5252, and *Hubble Space Telescope* (*HST*) Faint Object Spectrograph (FOS) spectra of the nucleus and two bright knots located 0'36 NE and 0'31 SW from it, show that the nuclear region exhibits the characteristics of a Liner with exceptionally strong [O I] emission, all lines being broad (FWHM  $\sim 1\,100\text{ km s}^{-1}$ ), while the gas outside the nucleus has a typical Seyfert 2 spectrum with relatively narrow lines ( $\sim 200\text{--}300\text{ km s}^{-1}$ ). We suggest that all the emitting gas is photoionized by the hidden non-thermal nuclear source detected through near-infrared (Kotilainen & Prieto 1995) and X-ray (Cappi et al. 1996) observations, the ionizing continuum, in the case of the central Liner, being “filtered” by a matter-bounded highly ionized cloud, hidden from our view by the same material obscuring the central continuum source.

**Key words:** galaxies: active – galaxies: nuclei – galaxies: Seyfert – galaxies: individual: NGC 5252

## 1. Introduction

NGC 5252 (1335+04) is a S0 galaxy at a redshift of  $z \sim 0.023$ . Nuclear spectra have shown it to be a Seyfert 2 galaxy (Véron-Cetty & Véron 1986; Huchra & Burg 1992). However, Osterbrock & Martel (1993) have found a weak broad  $H\alpha$  component in the nuclear region; Acosta-Pulido et al. (1996) have confirmed the presence of this broad component, with a measured FWHM of  $2\,485 \pm 78\text{ km s}^{-1}$ . Using a 3''-diameter aperture, Ruiz et al. (1994) detected the He I  $\lambda 1.083\ \mu\text{m}$  emission line in the nucleus; in addition to a narrow component ( $527\text{ km s}^{-1}$  FWHM), this line shows a broad feature ( $1\,043\text{ km s}^{-1}$  FWHM), which was interpreted as the signature of a Seyfert 1 cloud. Goodrich et al. (1994) have reported a marginal detection of a broad Pa  $\beta$  line.

Send offprint requests to: A.C. Gonçalves,  
(e-mail: anabela@obs-hp.fr)

<sup>★</sup> Based on observations collected at the Observatoire de Haute-Provence (CNRS, France) and *Hubble Space Telescope* data obtained from the Space Telescope European Coordinating Facility (ST-ECF) Archive.

**Table 1.** OHP and *HST* observing log

ID Label	Target	Date	Exposure Time (s)	
Y2YZ010BT	Nucleus	17.01.96	1 000	<i>HST</i>
Y2YZ010CT	NE knot	17.01.96	1 190	<i>HST</i>
Y2YZ010ET	SW knot	17.01.96	1 600	<i>HST</i>
NGC 5252 $H\beta$		06.03.97	1 200	OHP
NGC 5252 $H\alpha$		09.03.97	1 200	OHP

Unger et al. (1987), having obtained a high resolution (0.75 Å) slit spectrum of the nuclear region of NGC 5252, found the [O III]  $\lambda\lambda 4959, 5007$  lines to be double with a velocity separation of  $\sim 180\text{ km s}^{-1}$ . Acosta-Pulido et al. (1996) obtained a 2.0 Å resolution spectrum centered on the nucleus; this spectrum, covering the red spectral region, was extracted on a length of 4'6 along the slit, which was 1'0 wide. The [S II]  $\lambda\lambda 6716, 6731$  and  $H\alpha + [\text{N II}] \lambda\lambda 6548, 6584$  complexes were fitted with two Gaussians for each line, the velocity difference between the two components being  $\sim 200\text{ km s}^{-1}$ ; the need for an additional broad  $H\alpha$  component was already mentioned above.

Images taken in the light of the [O III]  $\lambda 5007$  line reveal a sharply defined biconical structure extending to a maximum radius of 48'', corresponding to 32 kpc, if  $H_0 = 50\text{ km s}^{-1}\text{ Mpc}^{-1}$  (Tadhunter & Tsvetanov 1989). Spectra (Durret & Warin 1990) and images in the light of [O III]  $\lambda 5007$  and  $H\alpha + [\text{N II}]$  (Haniff et al. 1991; Prieto & Freudling 1996) show that the gas outside the nucleus has a very high  $\lambda 5007/H\beta$  ratio. *HST* narrow band images show that three bright knots dominate the line emission in the innermost 1''; they are aligned along PA  $\sim 35^\circ$  with a total separation of  $\sim 0'7$  and are embedded in fainter diffuse gas (Tsvetanov et al. 1996).

J, H and K imaging with a seeing of 1'5–1'7 suggests the presence, in the nucleus, of a heavily reddened ( $A_V \sim 6$  mag) non stellar source (Kotilainen & Prieto 1995). ASCA observations show that NGC 5252 is a relatively strong X-ray source ( $L_{X(0.7-10\text{keV})} = 2.6 \cdot 10^{43}\text{ erg s}^{-1}$ ). A description of the spectrum with a single power law is ruled out; there is evidence for a strong soft excess. The best-fit partial covering model results in a flat ( $\Gamma \sim 1.45 \pm 0.2$ ) power-law continuum emitted by a source almost completely covered (at  $\sim 94\text{--}97\%$ ) by neutral

**Table 2.** Line profile fitting results for the OHP and *HST* spectra. Fluxes are in units of  $10^{-16}$  erg cm $^{-2}$  s $^{-1}$ . FWHMs have been corrected for instrumental broadening

	F(H $\alpha$ )	$\frac{\lambda 6584}{\text{H}\alpha}$	$\frac{\lambda 6300}{\text{H}\alpha}$	V (km s $^{-1}$ )	FWHM (km s $^{-1}$ )	F(H $\beta$ )	$\frac{\lambda 5007}{\text{H}\beta}$	V (km s $^{-1}$ )	FWHM (km s $^{-1}$ )
OHP	84	1.05	0.26	141	165	57	7.04	96	200
	231	0.90	0.29	-116	265	66	8.38	-146	225
	153	0.90	0.73	-261	1 460	66	3.59	-134	1 080
<i>HST</i> (SW knot)	19	1.03	0.29	114	230	5	7.09	99	210
<i>HST</i> (NE knot)	40	0.88	0.26	-240	340	7	11.11	-235	305
<i>HST</i> (Nucleus)	50	1.44	1.35	-124	530	21	3.58	-182	580
	137	0.63	0.49	-427	1 590	36	2.72	-501	1 760
OHP - <i>HST</i> (Nuc)	101	1.01	0.23	132	195	68	6.73	96	240
	189	0.82	0.19	-124	225	66	8.39	-151	245

matter ( $N_{\text{H}} \sim 4.3 \cdot 10^{22}$  cm $^{-2}$ ) (Cappi et al. 1996). For galactic X-ray sources, the hydrogen column density  $N_{\text{H}}$  and the visual extinction  $A_{\text{V}}$  follow the relation:  $A_{\text{V}} \sim 5 \cdot 10^{-22} N_{\text{H}}$  (Gorenstein 1975; Reina & Tarengi 1973). If this is valid for galactic nuclei, the observed X-ray extinction would imply a visual extinction of  $\sim 20$  mag. Although this is significantly larger than the value derived from near IR observations, it confirms that the nuclear source is heavily reddened. Spectropolarimetry allowed only a marginal detection of a broad H $\alpha$  component (Young et al. 1996).

The presence of a broad H $\alpha$  component in a Seyfert galaxy in which the nucleus is heavily obscured was surprising and induced us to observe this object.

## 2. Observations and data analysis

### 2.1. Observations

NGC 5252 was observed on March 6 and 9, 1997 with the spectrograph CARELEC (Lemaître et al. 1989) attached to the Cassegrain focus of the Observatoire de Haute-Provence 1.93m telescope. The detector was a 512 $\times$ 512 pixel, 27 $\times$ 27  $\mu\text{m}$  Tektronic CCD. We used a 600 l mm $^{-1}$  grating giving a dispersion of 66  $\text{\AA}$  mm $^{-1}$ . A Schott GG 435 filter was used in the red spectral range,  $\lambda\lambda$  6305–7215  $\text{\AA}$ ; the wavelength range covered in the blue was  $\lambda\lambda$  4825–5730  $\text{\AA}$ .

The slit width was 2''0, corresponding to a projected slit width on the detector of 50  $\mu\text{m}$  or 1.9 pixel; the slit P.A. was 90° for the blue spectrum and 180° for the red one. In each case, the galaxy nucleus was centered on the slit and 3 columns of the CCD ( $\sim 3''2$ ) were extracted. The seeing was  $\sim 3''$  on both nights; the resolution, as measured on the night sky emission lines, was  $\sim 3.5$   $\text{\AA}$  FWHM in the blue, and  $\sim 3.0$   $\text{\AA}$  FWHM in the red regions. The spectra were flux calibrated using the standard star Feige 66 (Massey et al. 1988), also used to correct the observations for the atmospheric absorption.

To supplement our own observations, we searched the *HST* archives for spectra of the central region of NGC 5252. Three FOS (description by Ford & Hartig 1990) spectra were retrieved, corresponding to the nucleus and the two knots located

0'36 NE and 0'31 SW from it (details are given in Table 1). All three *HST* spectra were obtained under the same setting conditions, with the G570H grating (4.37  $\text{\AA}$  diode $^{-1}$ ) and the FOS/RED detector (a 512 diodes linear array), resulting in a spectral range of  $\sim \lambda\lambda$  4570–6820  $\text{\AA}$ ; a single 0'26-diameter circular aperture was used. The spectra were submitted to the usual processes of substepping and overscanning, resulting in a 2 064 pixel coverage. Since each diode corresponds to 0'31 in the dispersion direction, the resolution was estimated at about 3.7  $\text{\AA}$  FWHM. The *HST* data were processed by the calibration pipeline *Calfos*, which includes flat-fielding, subtraction of the background and sky, and wavelength and flux calibrations. All (*HST* and OHP) spectra were deredshifted to rest wavelengths with  $z = 0.023$ .

The observing log is given in Table 1.

### 2.2. Data analysis

The presence of an old star population with many strong absorption lines can make the line fitting analysis difficult, especially in the blue spectral region. Bica (1988) has shown this old star population to have similar spectra in all Morgan (1958, 1959) classes; therefore, a suitable fraction of the spectra of the elliptical galaxies NGC 5982 and NGC 4365 (used as templates for the blue and red spectra, respectively) was subtracted from the observations to remove the old stellar population contribution. NGC 5982 was observed on March 6, 1997 with the same instrumental setting used for NGC 5252, while NGC 4365 was observed on February 28, 1984 with the Boller & Chivens spectrograph and the Image Dissector Scanner attached to the Cassegrain focus of the ESO 3.6 m telescope at La Silla; the dispersion was 59  $\text{\AA}$  mm $^{-1}$  and the resolution, 4.5  $\text{\AA}$  FWHM. The subtraction of these template spectra from our observations resulted in much smoother continua and corrected the flux of the Balmer emission lines for the underlying Balmer absorption.

Inspection of our two-dimensional spectra shows the lines to be double and spatially extended in the nuclear region, confirming earlier results. *HST* and OHP spectra were analysed in terms of Gaussian components, as described in Véron et al. (1997). The emission lines H $\alpha$ , [N II] $\lambda\lambda$  6548, 6584, [S II] $\lambda\lambda$

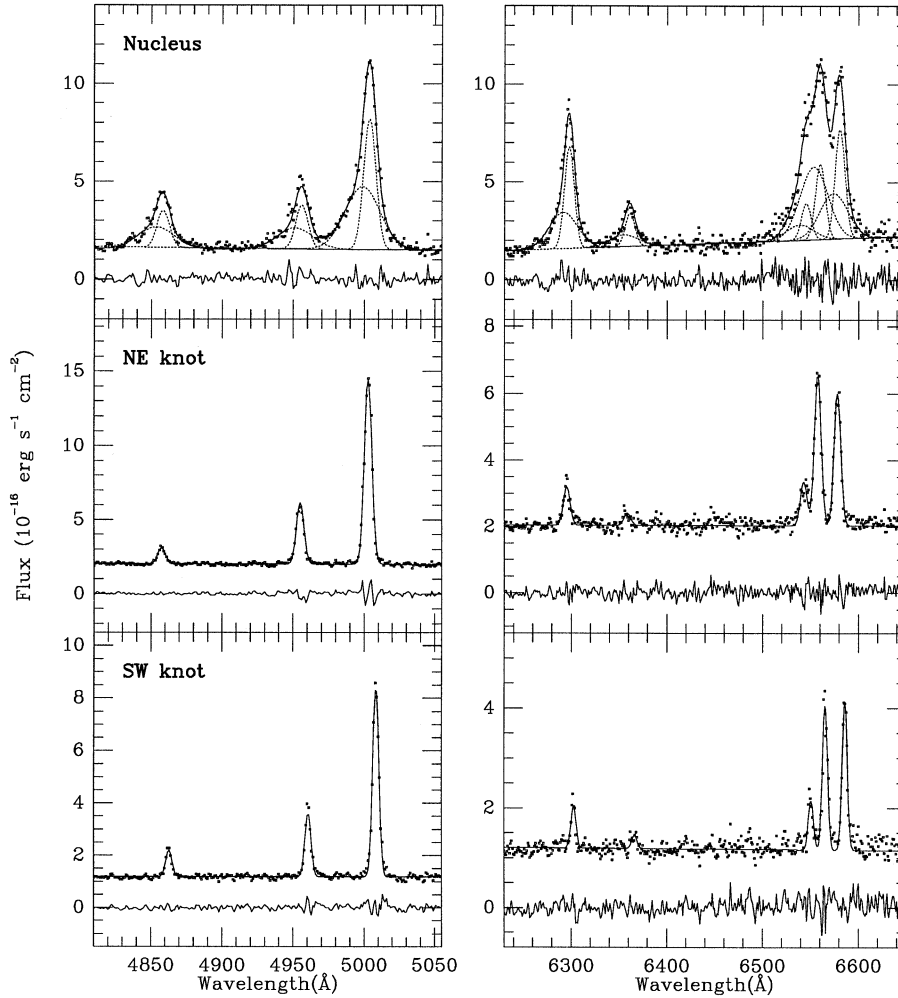


**Fig. 1.** Rest-wavelength *HST* spectra of the nucleus and knots, showing the spectral regions around  $H\beta$  and  $H\alpha$ . The data points are represented as small squares and the best fit as a solid line; the lower line shows the residuals. On the upper panels (spectra of the nucleus), the individual components are also drawn. All spectra were shifted upwards, so the continuum and residuals do not overlap; the origin of the vertical (flux) scales are, therefore, arbitrary

6716, 6731 and  $[O\text{I}]\lambda\lambda 6300, 6363$  (or  $H\beta$  and  $[O\text{III}]\lambda\lambda 4959, 5007$ ) were fitted by one or several sets of seven (three) Gaussian components; the width and redshift of each component in a set were taken to be the same. Therefore, in addition to the line intensities, the free parameters for each set of lines are one width and one redshift. The intensity ratios of the  $[N\text{II}]\lambda\lambda 6548, 6584$ ,  $[O\text{III}]\lambda\lambda 4959, 5007$  and  $[O\text{I}]\lambda\lambda 6300, 6363$  lines were taken to be equal to 3.00, 2.96 and 3.11, respectively (Osterbrock 1974).

Fitting our large aperture red spectrum with two sets of Gaussians gives unsatisfactory results, with large residuals not only for the  $H\alpha + [N\text{II}]$  complex, but also for the  $[O\text{I}]$  lines, which have an obvious blue wing. The best solution is not obtained by adding a broad  $H\alpha$  component, but rather a third set of Gaussians. This third set of components has a relatively broad width ( $\sim 1460\text{ km s}^{-1}$ ),  $\lambda 6584/H\alpha = 0.90$  and extremely strong  $[O\text{I}]$  lines ( $\lambda 6300/H\alpha = 0.73$ ). We obtained only an upper limit to the strength of the broad component of the  $[S\text{II}]$  lines; while the total  $[S\text{II}]$  flux relative to  $H\alpha$  for the two narrow components is 1.2 and 0.9 respectively, this ratio is  $< 0.5$  for the broad component. The same model, with three sets of components, also succeeds in matching the blue spectrum, one set having a large width ( $\sim 1080\text{ km s}^{-1}$ ) and  $\lambda 5007/H\beta = 3.59$ . The width found

for the  $H\alpha$  component is much larger than that of the equivalent  $H\beta$  line; this, however, may not be significant since the errors in the  $H\alpha$  width should be larger, the narrow  $H\alpha$  and  $[N\text{II}]$  components having a considerable relative strength. This “broad” line component has the characteristics of a Liner, while the two “narrow” line components are Seyfert 2-like, with weak  $[O\text{I}]$  lines and strong  $[O\text{III}]$  emission (see Table 2). Although the width of the “broad” component may seem large for a Seyfert 2 or a Liner, it is not exceptional as the line width of the prototype Seyfert 2 galaxy NGC 1068 is  $\sim 1500\text{ km s}^{-1}$  (Marconi et al. 1996).

We found no evidence for the presence of broad Balmer components typical of Seyfert 1 nuclei. The broad  $H\alpha$  component observed by Osterbrock & Martel (1993) and Acosta-Pulido et al. (1996) does not really seem to exist; this feature is rather due to the unresolved blend of the  $H\alpha$  and  $[N\text{II}]$  components. Whittle (1985) has mentioned the possibility of misidentifying weak relatively broad wings to the  $H\alpha$  and  $[N\text{II}]$  lines with a broad ( $\sim 2000\text{ km s}^{-1}$ )  $H\alpha$  component; we have an illustration of such a possibility in IRAS 13197–1627: Agüero et al. (1994) have fitted  $H\beta$  and the  $H\alpha + [N\text{II}]$  complex with a set of narrow Gaussian components, adding a broad component

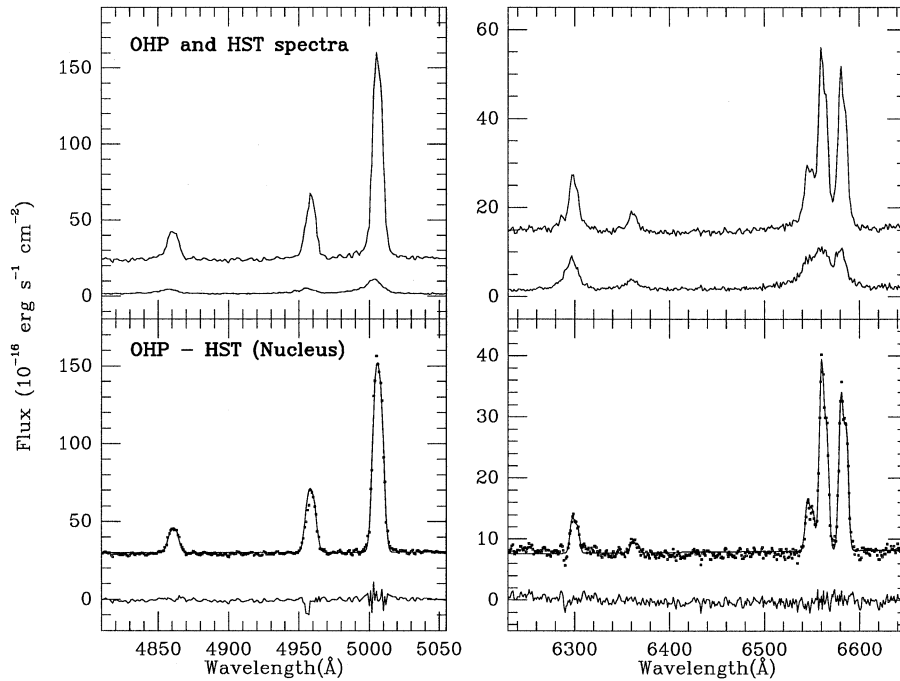


**Fig. 2.** The upper panels show the larger aperture OHP spectra (upper curves) and the *HST* nuclear spectra (lower curves), at rest-wavelengths. The lower panels show the difference of the two spectra (small squares), the best fit with two sets of narrow components (solid line) and the residuals (lower solid line). The spectra in the lower panel were shifted upwards by an arbitrary amount for clarity

to the Balmer lines; however, Young et al. (1996) showed that the  $H\alpha + [N II]$  complex can be very satisfactorily fitted by two sets of Gaussians (with FWHMs of 400 and 1350  $\text{km s}^{-1}$  and a  $\lambda 6584/H\alpha$  ratio of 1.94 and 1.35, respectively) without adding a broad  $H\alpha$  component.

Fitting the *HST* spectra showed that both the NE and SW knots (Fig. 1) have Seyfert 2-like spectra with relatively narrow lines ( $\sim 325$  and  $220 \text{ km s}^{-1}$  FWHM respectively, corrected for the instrumental broadening) and a velocity difference of  $\sim 345 \text{ km s}^{-1}$  (the SW knot being redshifted with respect to the NE knot). The observed line ratios are  $\lambda 5007/H\beta = 11.11$  (7.09),  $\lambda 6300/H\alpha = 0.26$  (0.29) and  $\lambda 6584/H\alpha = 0.88$  (1.03) for the NE (SW) knot, respectively. The nucleus spectrum (Fig. 1) is quite different: the lines are broad and have a complex profile; they have been fitted with two sets of components and have line ratios typical of Liners (see Table 2).

Our larger aperture ( $2'' \times 3''$ ) included both the nucleus and the two bright knots (Fig. 2, upper panels). Subtracting the *HST* nucleus spectrum from our own, without any scaling, resulted in a spectrum which is well fitted by a set of two narrow components (Fig. 2, lower panels) showing that the broad lines come exclusively from the small  $0''.26$  aperture centered on the nucleus. The velocity difference between the two narrow line systems in the resulting spectrum is  $\sim 250 \text{ km s}^{-1}$ , the FWHM is approximately the same in both systems ( $\sim 225 \text{ km s}^{-1}$ ) and the line ratios ( $\lambda 5007/H\beta = 8.39$  (6.73),  $\lambda 6300/H\alpha = 0.19$  (0.23) and  $\lambda 6584/H\alpha = 0.82$  (1.01) for the blueshifted and redshifted components, respectively) are very similar to those measured on the bright knots. The sum of the  $H\alpha$  fluxes of the two knots is equal to  $\sim 20\%$  of the total  $H\alpha$  flux measured on the differential (OHP – *HST*) spectrum, confirming the finding of Tsvetanov et al. (1996), that the knots are embedded in faint diffuse gas.

### 3. Discussion and conclusions

The ionization mechanism within Liners is still a subject of debate, mainly because their emission line spectrum can be reasonably reproduced by very different models, based on shock excitation, hot stars, or non-stellar photoionization. It has been shown that Liners and Seyfert 2 galaxies could be photoionized by the same non-thermal continuum, with a lower ionization parameter for Liners. The ionization parameter  $U$  ( $U = Q / (4\pi r^2 c n_e)$ ) is the number of available ionizing photons by hydrogen atom ( $Q$  is the number of Lyman continuum photons emitted by the source per second,  $r$  the distance of the emitting gas from the source,  $n_e$  the electron density of the cloud and  $c$  the speed of light). Ferland & Netzer (1983) showed that Seyfert 2s correspond to  $U \sim 3 \cdot 10^{-3}$  and Liners to  $U \sim 3 \cdot 10^{-4}$ .

Halpern & Steiner (1983) suggested that dilution of the input continuum could be obtained if cold clouds with column density  $N_H = 10^{22} \text{ cm}^{-2}$ , typical of broad-line clouds in Seyfert 1 galaxies, were covering a fraction  $f$  of the continuum as seen from the narrow-line region. The effect of covering is almost equal to a decrease in the ionization parameter  $U$  by a factor  $(1-f)$ . Liner spectra would be obtained for  $f \sim 0.90-0.98$ . Schultz & Fritsch (1994) and Binette et al. (1996) have proposed very similar models to produce Liner spectra in which an average AGN continuum is distorted or “filtered” by matter-bounded clouds, hidden from view by obscuring material. An intervening ionized cloud with  $\log N_H = 20$  would reduce the ionization parameter by a factor of  $\sim 10$ . Binette et al. argue that, in these models, the predicted  $\text{He II } \lambda 4686/H\beta$  ratio is  $< 0.01$ , in agreement with the fact that no reliable detection of He II has been reported in Liners, while if  $U$  is simply reduced, as proposed in the Halpern & Steiner model, without altering the shape of the ionizing spectrum, the expected  $\lambda 4686/H\beta$  ratio

is  $\sim 0.15$ . In the case of NGC 5252, the He II line could not be firmly detected on the *HST* nucleus spectrum; nevertheless, an upper limit to the relative flux of this line to H $\beta$  can be estimated at  $\sim 0.10$ , which does not allow us to decide between the two models.

In NGC 5252, a Seyfert 2 and a Liner are simultaneously present. Both near-IR and X-ray observations reveal the presence of an obscured non-stellar nuclear source. This source is most probably responsible for the ionization of the Seyfert 2 nebulosity. We suggest that the Liner is also ionized by this nuclear source, attenuated by an intervening matter-bounded cloud hidden from view by the same material which obscures the nuclear source; the “filtering” material would only partially cover the ionizing source, the Seyfert 2 clouds “seeing” directly this source without any intervening matter.

*Acknowledgements.* This research has made use of the NASA/IPAC extragalactic database (NED), which is operated by the Jet Propulsion Laboratory, Caltech, under contract with the National Aeronautics and Space Administration. A.C. Gonçalves acknowledges support from the *Junta Nacional de Investigação Científica e Tecnológica*, Portugal, during the course of this work (PhD. grant PRAXIS XXI/BD/5117/95).

## References

- Acosta-Pulido J.A., Vila-Vilaro B., Perez-Fournon I., Wilson A.S., Tsvetanov Z.I., 1996, *ApJ* 464, 177
- Aguero E.L., Calderon J.H., Paolantonio S., Boedo E.S., 1994, *PASP* 106, 978
- Bica E., 1988, *A&A* 195, 76
- Binette L., Wilson A.S., Storchi-Bergman T., 1996, *A&A* 312, 365
- Cappi M., Mihara T., Matsuoka M. et al., 1996, *ApJ* 456, 141
- Durret F., Warin F., 1990, *A&A* 238, 15
- Ferland G.J., Netzer H., 1983, *ApJ* 264, 105
- Ford H.C., Hartig G.F., 1990, *Faint Object Spectrograph Instrument Handbook*, Baltimore (STScI)
- Goodrich R.W., Veilleux S., Hill G.J., 1994, *ApJ* 422, 521
- Gorenstein P., 1975, *ApJ* 198, 95
- Halpern J.P., Steiner J.E., 1983, *ApJ* 269, L37
- Haniff C.A., Ward M.J., Wilson A.S., 1991, *ApJ* 368, 167
- Huchra J.P., Burg R., 1992, *ApJ* 393, 90
- Kotilainen J.K., Prieto M.A., 1995, *A&A* 295, 646
- Lemaître G., Kohler D., Lacroix D., Meunier J.-P., Vin A., 1989, *A&A* 228, 546
- Marconi A., van der Werf P.P., Moorwood A.F.M., Oliva E., 1996, *A&A* 315, 335
- Massey P., Strobel K., Barnes J.V., Anderson E., 1988, *ApJ* 328, 315
- Morgan W.W., 1958, *PASP* 70, 364
- Morgan W.W., 1959, *PASP* 71, 394
- Osterbrock D.E., 1974, *Astrophysics of gaseous nebulae*. Freeman and company, San Francisco
- Osterbrock D.E., Martel A., 1993, *ApJ* 414, 552
- Prieto M.A., Freudling W., 1996, *MNRAS* 279, 63
- Reina C., Tarenghi M., 1973, *A&A* 26, 257
- Ruiz M., Rieke G.K., Schmidt G.D., 1994, *ApJ* 423, 608
- Schultz H., Fritsch C., 1994, *A&A* 291, 713
- Tadhunter C., Tsvetanov Z.I., 1989, *Nat.* 341, 422
- Tsvetanov Z.I., Morse J.A., Wilson A.S., Cecil G., 1996, *ApJ* 458, 172
- Unger S.W., Pedlar A., Axon D.J. et al., 1987, *MNRAS* 228, 671
- Véron-Cetty M.-P., Véron P., 1986, *A&AS* 65, 241
- Véron P., Gonçalves A.C., Véron-Cetty M.-P., 1997, *A&A* 319, 52
- Whittle M., 1985, *MNRAS* 216, 817
- Young S., Hough J.H., Efstathiou A. et al., 1996, *MNRAS* 281, 1206